



DETERMINATION OF THE NEUTRINO FLUX WITH PERFECT FOCUSING

David C. Carey

October 10, 1972

I. Introduction

An important consideration in the design and construction of the NAL neutrino facility¹⁻¹⁷ over the past several years has been the expected flux of neutrinos through a detector. Interesting questions concern the dependence of the neutrino flux at a given energy on the decay tunnel diameter and length, the shield length, the detector size, the proton beam energy, the target dimensions, the particle production model, and the focusing devices used. Certain of these factors may be studied relatively independently of others. A thorough evaluation of the effects of target dimensions has been done by Stevenson.¹⁸

The optimal set of focusing elements for a neutrino facility of given dimensions may be a function of those dimensions. It is desirable therefore to be able to study the effect of changes in various facility dimensions or the particle production model, independently of any particular focusing device.

The concept of perfect focusing has proven to be a useful tool for this purpose. Immediately following the target is assumed to be a "perfect" focusing device which causes all mesons emitted by the target to travel down the axis of the decay tunnel. The mesons decay with a fixed probability per



unit proper time until they reach the end of the tunnel. We are thus free from considerations of the focusing device used or the tunnel diameter.

In planning an experiment using a wide band focusing device, one can obtain a rough estimate of the expected flux by assuming it to be a fixed fraction of that obtainable with perfect focusing.

Because of the simple nature of perfect focusing it is possible to express the expected flux at a given neutrino energy in a simple form. We thus avoid both the tedium and inaccuracies of ray tracing. The limitations of ray-tracing methods and the need for a new approach in cases involving small solid angles were first pointed out by Kang.¹⁹

In Section II below we describe the layout of the neutrino facility and the kinematics of the meson decay which produces the neutrinos. In Section III we develop the formalism used to calculate the expected neutrino flux versus neutrino energy. Finally in Section IV we present some sample results and make a comparison with those that would be obtained by ray tracing.

II. Layout and Kinematics

The general layout of the NAL neutrino facility is illustrated in Figure 1. The incoming proton beam strikes the target, as shown, from the left. The number of protons which interact in the target depends on both the target size and its material. The secondary particles created, along with the remains of the original proton beam, then proceed down the decay tunnel. The

positively charged pions and kaons decay, producing neutrinos. In both cases the most important decay mode is that which produces a μ^+ and a neutrino. For pions the branching ratio into this mode is essentially 100% while for kaons it is 63.8%.

The decay takes place isotropically in the meson center of mass, the neutrino proceeding in a straight line which may or may not intersect the detector. We are interested in determining the number of neutrinos whose paths do indeed hit the detector.

If we let m be the mass of the meson, μ that of the muon, and \bar{E}_ν and $\bar{\phi}$ be the center of mass neutrino energy and decay angle respectively, then we have:

$$m = \sqrt{\bar{E}_\nu^2 + \mu^2} + \bar{E}_\nu \quad (1)$$

Solving for \bar{E}_ν gives:

$$\bar{E}_\nu = \frac{m^2 - \mu^2}{2m} = \frac{m}{2} r \quad (2)$$

where we define the quantity r by:

$$r = \frac{m^2 - \mu^2}{m^2}$$

The longitudinal and transverse components of the neutrino momentum in the center of mass are then given by:

$$\begin{aligned} \bar{p}_{\nu\ell} &= \frac{m}{2} r \cos \bar{\phi} \\ \bar{p}_{\nu t} &= \frac{m}{2} r \sin \bar{\phi} \end{aligned} \quad (4)$$

Now if we let p and E represent the lab momentum and energy of the meson we have for the laboratory components of the neutrino momentum:

$$p_{\nu\ell} = \frac{r}{2} \left[E \cos \bar{\phi} + p \right]$$

$$p_{\nu t} = \frac{m}{2} r \sin \bar{\phi} \quad (5)$$

while the laboratory decay angle ϕ is given by:

$$\tan \phi = \frac{m \sin \bar{\phi}}{E \cos \bar{\phi} + p} \quad (6)$$

If we take the high energy limit, and express the laboratory decay angle in terms of the laboratory neutrino energy we get:

$$E_{\nu} = \frac{p}{r} \frac{1}{2} \left[1 + \cos \bar{\phi} \right]$$

$$\phi = \frac{m}{p} \left[(rp - E_{\nu}) / E_{\nu} \right]^{\frac{1}{2}} \quad (7)$$

We see that the quantity r is the maximum fraction of the laboratory meson momentum that the neutrino may possess. Because the center of mass distribution is uniform in $\cos \bar{\phi}$, the laboratory neutrino energy distribution will be uniform from zero to a maximum of rp .

The laboratory distribution of decays will still be isotropic in azimuthal angle. The neutrinos of a given energy produced by a decaying meson therefore form a cone with half angle given by equation (7). The fraction of the cone intersecting the detector equals the fraction of neutrinos of a given energy passing through the detector. With perfect focusing the cone either entirely hits or misses the detector, rendering the calculations particularly simple.

III. Determining the Flux

A. The Meson Production Spectrum

The meson production spectrum is typically expressed as the number of mesons produced per proton interaction per unit momentum

interval and solid angle, i.e., $d^2N/dp d\Omega$. In past calculations the CKP²⁰ and Hagedorn-Ranft²¹⁻²⁴ models were the most often employed, while others have, at times, been considered or used.²⁵⁻²⁹

It is convenient for numerical calculations to specify the production spectrum as a matrix S_{mn} . The momentum and angle ranges are divided into intervals and S_{mn} gives the total number of particles produced in the m'th momentum interval and the n'th angle interval. A given matrix element is given by:

$$S_{mn} = 2\pi \int_{\Delta\theta_n} \int_{\Delta p_m} \frac{d^2N}{dp d\Omega} \sin \theta dp d\theta \quad (8)$$

where Δp_m and $\Delta\theta_n$ represent the m'th momentum interval and n'th angle interval respectively.

If the target length is t and the interaction length for protons is λ_p , then the fraction of protons which interact in the target is given by:

$$f = 1 - e^{-t/\lambda_p} \quad (9)$$

The quantity S_{mn} gives the number of mesons produced per interacting proton. We now wish to take into account absorption of mesons in the target to determine an effective spectrum produced by the target. To do this we divide the target into ℓ parts, where the same number of proton interactions takes place in each part. In each section we determine a point at distance Q_i from the front of the target which similarly divides that section into two parts. The distance Q_i is then given by:

$$Q_i = -\lambda_p \log \left[1 - (i - \frac{1}{2}) f/\ell \right] \quad (10)$$

If the radius of the target is R then for small angles the path length travelled through the target by a meson produced at point Q_i and at angle θ_n is given approximately by:

$$d_{in} = \min \left[t - Q_i, R/\theta_n \right] \quad (11)$$

Since, with perfect focusing, the particles travel along the tunnel axis immediately after leaving the target, we are interested only in the number of mesons per given momentum interval. The effective momentum spectrum, or number of particles in the m 'th momentum interval per interacting proton, is given approximately by:

$$S_m = \frac{1}{\ell} \sum_{n,i} S_{mn} e^{-d_{in}/\lambda_m} \quad (12)$$

The quantity λ_m is the meson interaction length in the target. In practice we have always taken λ_m to be equal to λ_p .

As we shall see below, it is convenient to re-express the effective spectrum as an analytic expression for dN/dp , the number of particles produced per unit momentum interval. We use a polynomial of order two to represent the effective spectrum throughout the m 'th momentum interval, so that:

$$\left(\frac{dN}{dp} \right)_m = A_m + B_m p + C_m p^2 \quad (13)$$

There will be a different set of coefficients for each momentum interval. We choose values for these coefficients such that the integral of the polynomial for three given intervals equals the number of particles S_m for those intervals. For the lowest momentum interval the three given intervals are the lowest three. For the highest momentum interval the three given are the highest

three. For all others the three given intervals are the interval in question and the two adjacent. Given these three conditions we may form a matrix and solve for the three coefficients.

B. Energy Intervals and Geometry

We now determine the flux for a given neutrino energy E_ν . A table of neutrino flux versus neutrino energy may be obtained by repeating the procedure for different values of E_ν .

In perfect focusing the mesons all travel up the axis of the decay tunnel. Neutrinos of energy E_ν , produced at a given point by mesons of momentum p , form a cone whose axis coincides with that of the decay tunnel and with a half angle ϕ given by equation (7). Let the radius of the detector be b , the tunnel length be d , the shield length be s , and the recess distance (the distance from the shield to the detector) be r . Then if $\phi > b/(s + r)$, at no point will the decay cone intersect the detector and the neutrino flux will be zero. If $\phi < b/(d + s + r)$ then the neutrino cone will intersect the detector from all points in the tunnel. If $b/(s + r) > \phi > b/(d + s + r)$ then there will be a point in the decay tunnel before which no neutrinos will strike the detector and after which all will.

We now examine, for fixed E_ν , the behavior of ϕ as a function of p . A typical graph of ϕ versus p is given in Figure 2. The minimum meson momentum necessary to produce a neutrino of energy E_ν is E_ν/r . Below that momentum the angle ϕ is undefined. From zero at threshold the angle ϕ

rises to a maximum of $mr/2E_\nu$ at a meson momentum of $2E_\nu/r$ or twice the threshold momentum. From there it asymptotically again approaches zero.

Now if $\phi_{\max} < b/(d + s + r)$ the decay cone will intersect the detector from all points in the tunnel for all meson momenta. Letting L equal $d + s + r$ and a_1 be equal to mL/b , then this condition is equivalent to the condition $E_\nu \geq ra_1/2$. At lower neutrino energies there will be a meson momentum interval where not all neutrinos strike the detector. The limits p_1 and p_2 of this interval are given by:

$$p_{1,2} = \frac{ra_1^2}{2E_\nu} \left[1 \pm \sqrt{1 - \left(\frac{2E_\nu}{ra_1}\right)^2} \right] \quad (14)$$

As the neutrino energy decreases the maximum decay angle becomes larger and when $\phi_{\max} > b/(s + r)$ there appears a momentum interval where no neutrinos intersect the detector. This condition does not occur whenever we have $E_\nu \geq ra_2/2$ where a_2 is given by $m(s + r)/b$. When E_ν is below this critical energy the limits of the momentum interval in which no neutrinos hit the detector are given by:

$$p_{3,4} = \frac{ra_2^2}{2E_\nu} \left[1 \pm \sqrt{1 - \left(\frac{2E_\nu}{ra_2}\right)^2} \right] \quad (15)$$

In summary, when $E_\nu \geq ra_1/2$, there is a single meson momentum interval, in which all produced neutrinos strike the detector. For $ra_1/2 > E_\nu \geq ra_2/2$, we have three meson momentum intervals. In the first and third, all neutrinos produced strike the detector, while in the second only some of the neutrinos do so. Finally for $E_\nu < ra_2/2$, we have five meson momentum intervals. In the third the maximum of ϕ occurs and

no neutrinos strike the detector. For the second and fourth momentum intervals only some of the neutrinos strike the detector.

C. Integrals

We now set up the required integrals for each of the cases described above. If we let S equal dN/dp , the number of mesons per unit momentum interval, then the number of neutrinos per unit energy interval produced is S/rp . This is true as long as the meson momentum is above threshold for production of neutrinos of the given energy. The decay length is proportional to the meson momentum, so the fraction of mesons undecayed after a length ℓ is $e^{-\ell/C_D p}$, where C_D is a constant of proportionality.

Consider first a meson momentum interval in which all produced neutrinos of energy E_ν strike the detector. The total fraction of mesons decaying in the tunnel is given as $1 - e^{-d/C_D p}$, so that the number of neutrinos hitting the detector is given by the integral:

$$N_T = \int S \left[1 - e^{-d/C_D p} \right] \frac{1}{rp} dp \quad . \quad (16)$$

The integration is done over the momentum interval in question.

For larger decay angles ϕ , only a fraction of the neutrinos strike the detector. There then exists a distance from the tunnel end ℓ_{\min} where the decay cone begins to intersect the detector. This distance is given by:

$$\ell_{\min} = \frac{b}{\phi} - s - r \quad (17)$$

The number of neutrinos striking the detector from this momentum interval is now given by:

$$N_T = \int S e^{-d/C_D p} \left[e^{-\ell_{\min}/C_D} - 1 \right] \frac{1}{rp} dp \quad (18)$$

The total neutrino flux at a given energy for each of the three cases discussed above may now be expressed in terms of the integrals given. The threshold meson momentum for production of neutrinos of energy E_ν is E_ν/r which represents the lower limit on the first integral. The upper limit on the last integral, p_{\max} may, in practical cases, be taken to be somewhat less than the incident proton momentum.

For $E_\nu > ra_1/2$, we have a single momentum interval and the flux per unit neutrino energy is given by:

$$N_T = \int_{E_\nu/r}^{p_{\max}} S \left[1 - e^{-d/C_D p} \right] \frac{1}{rp} dp \quad (19)$$

In the case where $ra_1/2 > E_\nu > ra_2/2$, there are three relevant momentum intervals and the total neutrino flux is given by:

$$\begin{aligned} N_T = & \int_{E_\nu/r}^{p_1} S \left[1 - e^{-d/C_D p} \right] \frac{1}{rp} dp \\ & + \int_{p_1}^{p_2} S e^{-d/C_D p} \left[e^{\ell_{\min}/C_D} - 1 \right] \frac{1}{rp} dp \\ & + \int_{p_2}^{p_{\max}} S \left[1 - e^{-d/C_D p} \right] \frac{1}{rp} dp \quad . \quad (20) \end{aligned}$$

Finally when $E_\nu < ra_2/2$, there are five momentum intervals, but only four contributing any flux, giving:

$$N_T = \int_{E_\nu/r}^{p_1} S \left[1 - e^{-d/C_D p} \right] \frac{1}{rp} dp$$

$$\begin{aligned}
& + \int_{P_1}^{P_3} s e^{-d/C_D p} \left[e^{\ell_{\min}/C_D p} - 1 \right] \frac{1}{rp} dp \\
& + \int_{P_4}^{P_2} s e^{-d/C_D p} \left[e^{\ell_{\min}/C_D p} - 1 \right] \frac{1}{rp} dp \\
& + \int_{P_2}^{P_{\max}} s \left[1 - e^{-d/C_D p} \right] \frac{1}{rp} dp
\end{aligned} \tag{21}$$

It remains simply to evaluate these integrals. For purposes of representing the production spectrum we have divided the momentum range into M intervals and approximated S in each interval by a polynomial $A_m + B_m p + C_m p^2$. We must therefore evaluate the above integrals for each of the M momentum intervals separately using the expression for S appropriate to the given interval. We then sum over the results for all M intervals to obtain the total neutrino flux. The range of each integration is the intersection of that given above with the given momentum interval.

The three integrals to be evaluated are given by:

$$I_1 = \int_{P_a}^{P_b} s \frac{1}{rp} dp \tag{22}$$

$$I_2 = \int_{P_a}^{P_b} s e^{-d/C_D p} \frac{1}{rp} dp \tag{23}$$

$$I_3 = \int_{P_a}^{P_b} s e^{-(d - \ell_{\min})/C_D p} \frac{1}{rp} dp \tag{24}$$

We now replace S by its polynomial expression and drop subscripts. For the first integral we have:

$$I_1 = \frac{1}{r} \int_{p_a}^{p_b} \left[\frac{A}{p} + B + Cp \right] dp \quad (25)$$

$$= \frac{1}{r} \left[A \log (p_b/p_a) + B(p_b - p_a) + \frac{1}{2}C(p_b^2 - p_a^2) \right]$$

To evaluate the second we let $x = 1/p$ and $\lambda = d/C_D$. Then we have:

$$I_2 = \frac{1}{r} \int \left[A \frac{1}{x} + B \frac{1}{x^2} + C \frac{1}{x^3} \right] e^{-\lambda x} dx$$

$$= \frac{1}{r} \left\{ \left[A - \lambda B + \frac{1}{2} \lambda^2 C \right] \int \frac{e^{-\lambda x}}{x} dx \right.$$

$$\left. + \left[-B + \frac{1}{2} \lambda C \right] \frac{e^{-\lambda x}}{x} - \frac{1}{2} C \frac{e^{-\lambda x}}{x^2} \right|_{x_a}^{x_b} \quad (26)$$

where $x_a = 1/p_a$ and $x_b = 1/p_b$. The exponential integral is well known^{30,31} and may be expanded in any of several possible series, depending on the value of the argument.

The third integral may be rewritten as:

$$I_3 = \int_{p_a}^{p_b} \left[A + Bp + Cp^2 \right] \exp \left[\frac{b}{C_D m} \left(\frac{E_v}{rp - E_v} \right)^{\frac{1}{2}} \right] \exp \left[- \frac{L}{C_D p} \right]$$

$$\cdot \frac{1}{rp} dp \quad (27)$$

and is obviously a bit unwieldy for direct evaluation. Denoting the integrand as F(p) we can approximate the integral as a sum:

$$I_3 \approx \sum_{i=1}^N F(p_i) (\Delta p)_i \quad (28)$$

where $\{(\Delta p)_i\}$ is a partition of the interval $[p_a, p_b]$, and p_i is a point within the i 'th subinterval. The partition is chosen so that the intervals will be smallest where the variation of the integrand is largest. Since, in part of the integration range, the meson momentum may be near threshold for production of neutrinos of the given energy, the term which could have the most rapidly varying behavior is $\exp\left[\frac{b}{C_{Dm}} \left(\frac{E_\nu}{rp - E_\nu}\right)^{\frac{1}{2}}\right]$. We therefore divide the interval p_a, p_b in such a way that the change in this variable across each interval will be uniformly equal to 0.1. The total number of intervals is then given by:

$$N = \frac{10b}{C_{Dm}} \left[\left(\frac{E_\nu}{rp_a - E_\nu}\right)^{\frac{1}{2}} - \left(\frac{E_\nu}{rp_b - E_\nu}\right)^{\frac{1}{2}} \right] \quad (29)$$

We adjust this quantity so it is an exact integer, and to insure an adequate number of intervals, if it is less than ten, readjust it upwards to equal ten. Denoting the quantity in brackets in equation (29) as Δ , then we can define a quantity δ by:

$$\delta = \Delta/N \quad (30)$$

and a sequence g_i as:

$$g_i = \left(\frac{E_\nu}{rp_b - E_\nu}\right)^{\frac{1}{2}} + \left(i - \frac{1}{2}\right) \delta \quad (31)$$

We then have:

$$p_i = \frac{E_\nu}{r} \left(1 + \frac{1}{g_i^2}\right)$$

$$(\Delta p)_i = \frac{E_\nu}{r} \left(\frac{1}{(g_i - \frac{1}{2}\delta)^2} - \frac{1}{(g_i + \frac{1}{2}\delta)^2}\right) \quad (32)$$

giving the points and partition to be used to evaluate the sum in equation (28).

IV. Results

The above numerical methods were incorporated into the NAL neutrino flux program NUADA in August, 1970. This program has then been used for all subsequent calculations of perfect focusing.¹³⁻¹⁷

In Figure 3 we present the results of a sample calculation for both pions and kaons. The decay tunnel length is taken to be 395.5 meters, the shield to be 910 meters, the recess to be 100 meters, and the detector diameter to be 1.35 meters.³¹ A target one centimeter long and four millimeters in diameter is used. The mean free path for both protons and mesons is taken to be .3 meters. An incident proton energy of 500 GeV is assumed and the spectrum is Hagedorn-Ranft.

For comparison, we present in Figure 4 the same calculation done by ray-tracing methods. Consecutive points are joined by straight lines to illustrate the inaccuracy of the results.

References

1. L. Hyman, NAL 1968 Summer Study Report B.1-68-20.
2. Ugo Camerini and S. L. Meyer, NAL 1968 Summer Study Report B.1-68-79.
3. M. L. Stevenson, NAL 1968 Summer Study Report B.1-68-104.
4. Y. W. Kang, F. A. Nezrick, NAL 1969 Summer Study Report SS-146.
5. S. L. Meyer, T. Toohig, NAL 1969 Summer Study Report SS-139.
6. A. R. Kalbfleisch, NAL 1969 Summer Study Report SS-121.
7. D. H. Frisch, Y. W. Kang, NAL 1969 Summer Study Report SS-160.
8. Y. W. Kang, F. A. Nezrick, NAL 1969 Summer Study Report SS-142.
9. Y. W. Kang, M. L. Stevenson, NAL Report TM-217 (1970).
10. D. C. Carey, Y. W. Kang, F. A. Nezrick, R. J. Stefanski, M. L. Stevenson, NAL Report TM-220 (1970).
11. D. Carey, Y. W. Kang, F. A. Nezrick, R. J. Stefanski, NAL Report TM-221 (1970).
12. D. Carey, Y. W. Kang, F. A. Nezrick, R. J. Stefanski, NAL Report TM-222 (1970).
13. Y. Cho, NAL 1970 Summer Study Report SS-200.
14. R. A. Burnstein, NAL 1970 Summer Study Report SS-180.
15. R. B. Palmer, NAL 1970 Summer Study Report SS-209.
16. D. Carey, Y. W. Kang, F. A. Nezrick, R. J. Stefanski, J. K. Walker, NAL Report TM-265 (1970).
17. Y. W. Kang, F. A. Nezrick, NAL Report TM-299 (1971).
18. M. L. Stevenson, NAL Report TM-218 (1970).
19. Y. W. Kang, private communication.
20. G. Cocconi, L. J. Koester, D. H. Perkins, UCRL Report 10022, p. 167 (1961).

21. R. Hagedorn, Suppl. Nuovo Cimento 3, 147 (1965).
22. R. Hagedorn, J. Ranft, Suppl. Nuovo Cimento 6, 169 (1968).
23. R. Hagedorn, Suppl. Nuovo Cimento 6, 311 (1968).
24. M. Awschalom, T. White, NAL Report FN-191 (1969).
25. R. K. Adair, Phys. Rev. 172, 1370 (1968).
26. C. Risk, UCRL Report 20841 (1971).
27. C. Risk, J. Friedman, PRL 27, 353 (1971).
28. C. Risk, LBL Report 368 (1971).
29. M. L. Stevenson, NAL Report TM-318 (1971).
30. W. Magnus, F. Oberhettinger, R. P. Soni, Formulas and Theorems for the Special Functions of Mathematical Physics, Springer-Verlag, New York, 1966.
31. Milton Abramowitz, Irene A. Stegun, Handbook of Mathematical Functions, National Bureau of Standards, 1964.
32. F. A. Nezrick, private communication.

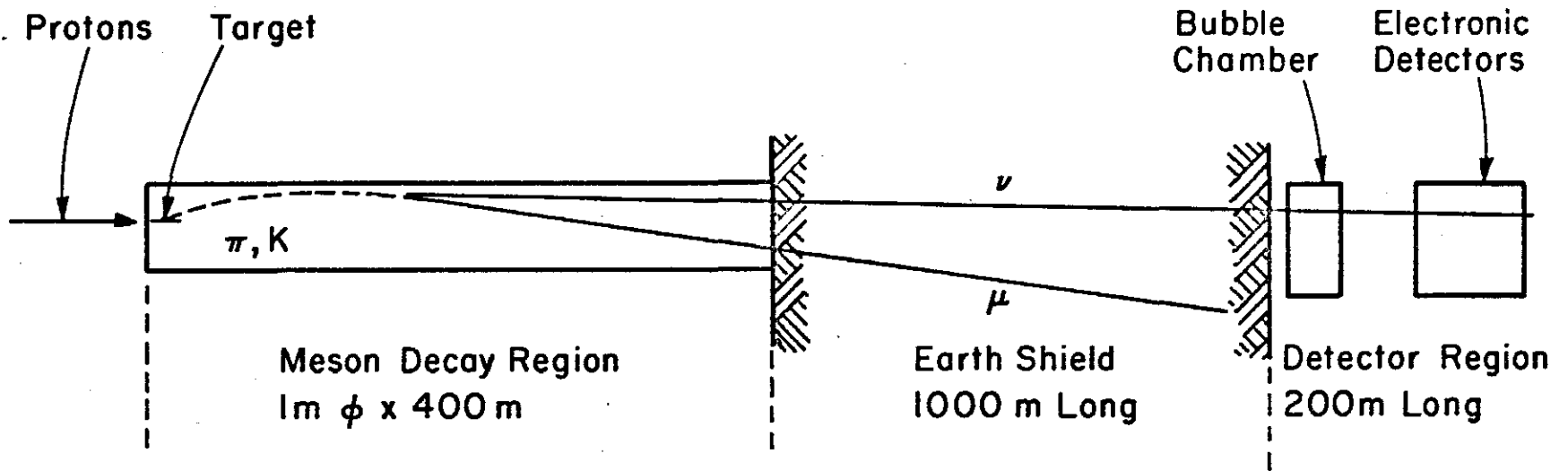


Figure 1: Layout of the NAL neutrino facility.

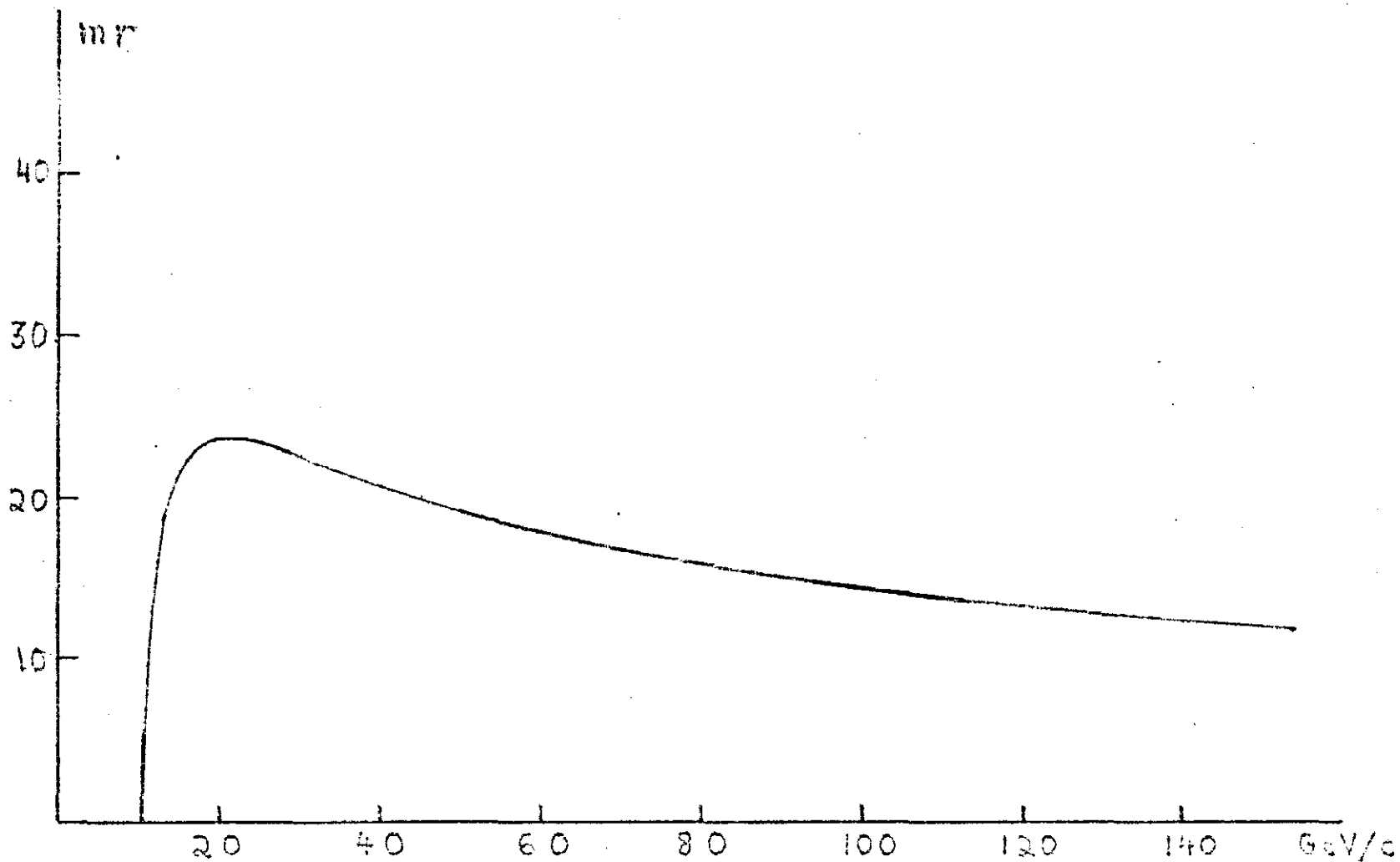


Figure 2: Neutrino decay angle versus meson momentum. The parent mesons in this case are kaons. The energy of the produced neutrino is 10 GeV. The angle is that made by the neutrino with the original meson direction in the laboratory system.

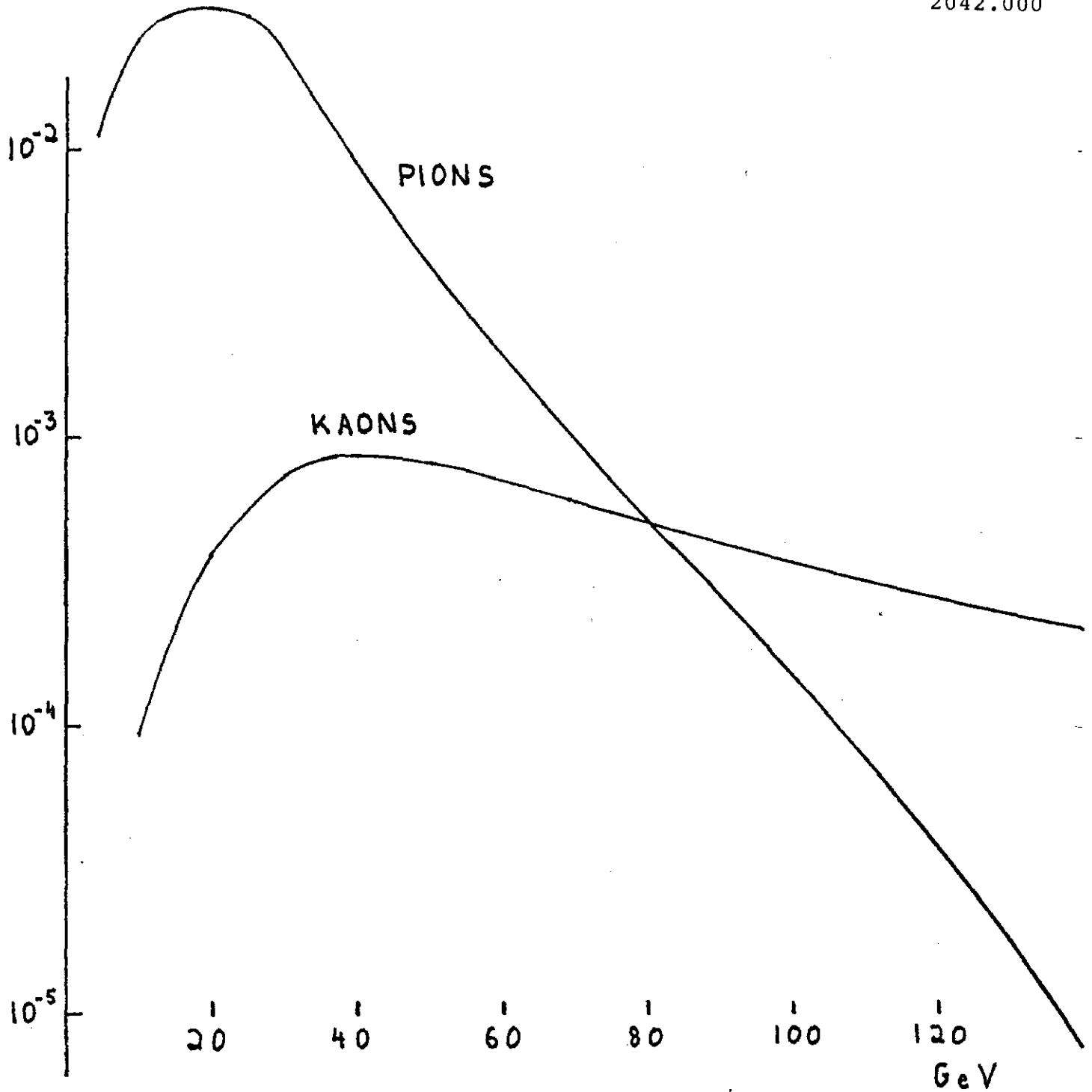


Figure 3: Neutrino flux versus neutrino energy. Method of calculation is that described in this paper. The ordinate is neutrinos/GeV - square meter - 10^4 incident protons.

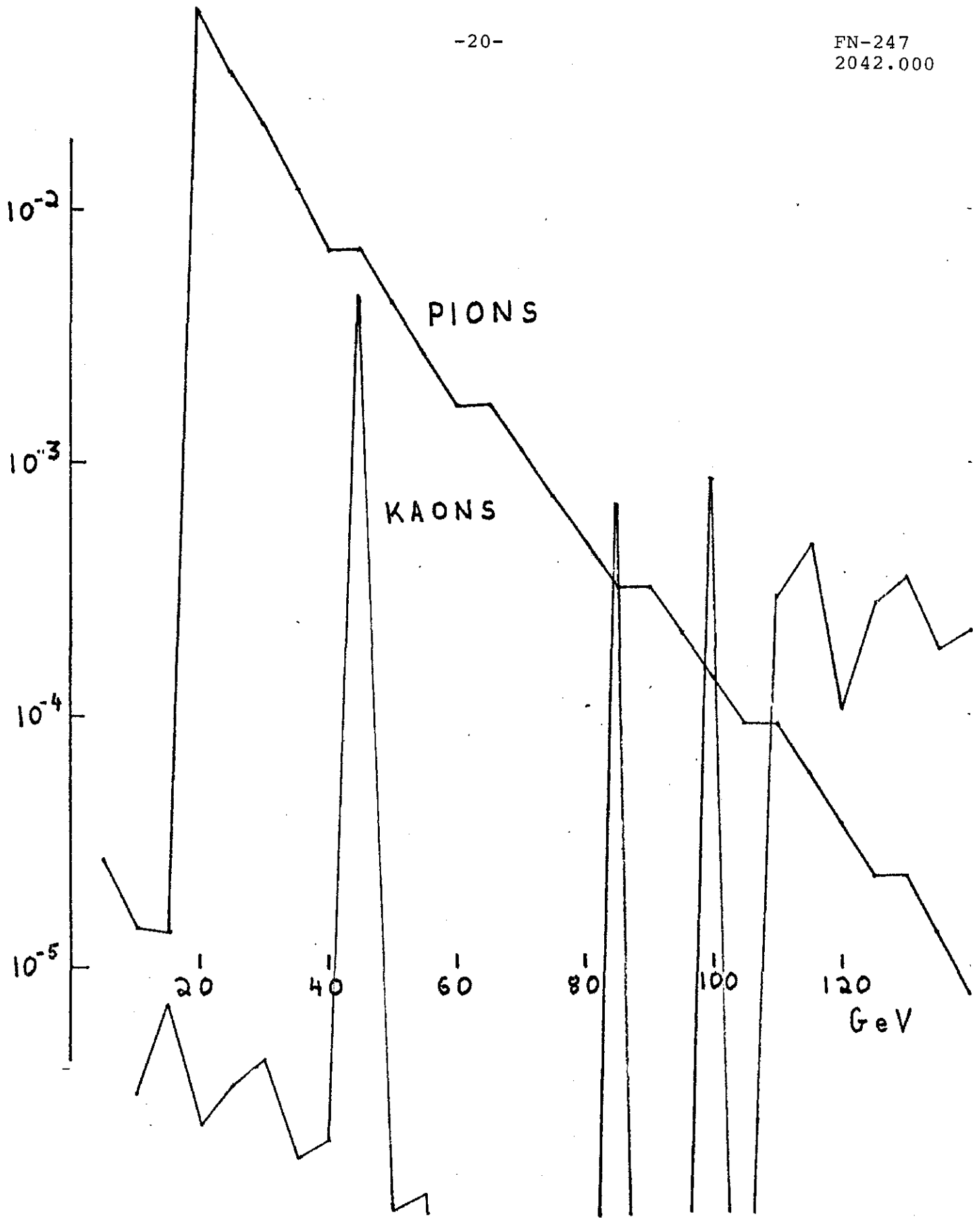


Figure 4: Same as Figure 3 using ray-tracing methods.